8-2023

Laser-Induced Forward Transfer (LIFT) based Bioprinting of the Collagen I with Retina Photoreceptor Cells

Md Shakil Arman

Ben Xu

Andrew Tsin

Jianzhi Li

Available online at www.sciencedirect.com

Manufacturing Letters

Manufacturing Letters 35 (2023) 477-484

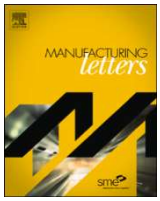

51st SME North American Manufacturing Research Conference (NAMRC 51, 2023)

Laser-Induced Forward Transfer (LIFT) based Bioprinting of the Collagen I with Retina Photoreceptor Cells

Md Shakil Arman[a], Ben Xu[b], Andrew Tsin[c], Jianzhi Li[a*]

[a]*Department of Manufacturing and Industrial Engineering, The University of Texas Rio Grande Valley, Edinburg, TX, 78539, USA*
[b]*Department of Mechanical Engineering, University of Houston , Houston, TX, 77204, USA*
[c]*Department of Molecular Science, The University of Texas Rio Grande Valley School of Medicine, Edinburg, TX, 78539, USA*

* Corresponding author. Tel.: +1-956-665-7329; *E-mail address:* jianzhi.li@utrgv.edu

Abstract

This study focuses on the 3D bioprinting of retina photoreceptor cells using a laser-induced forward transfer (LIFT) based bioprinting system. Bioprinting has a great potential to mimic and regenerate the human organoid system, and the LIFT technique has emerged as an efficient method for high-resolution micropatterning and microfabrication of biomaterials and cells due to its capability of creating precise, controlled microdroplets. In this study, the parameters for an effective femtosecond laser-based LIFT process for 3D bioprinting of collagen biomaterial were studied. Different concentrations of collagen I solutions were tested and 0.75 mg/ml to 1 mg/ml collagen I was identified as the right concentration that can be transferred through the LIFT system. Then, retinal cone cells were mixed with collagen I and Dulbecco's Modified Eagle's Medium (DMEM) and printed drop-by-drop lines. Some important laser parameters such as pulse energy and pulse pick divider were experimented with to form a successful, smooth, high-resolution deposition. The cell viability in the bioink and printed droplet was measured at different time horizons. A general full factorial design of the experiment was used to analyze and observe the relationship between the droplet quality and the LIFT process parameters. Using 15 µJ and 16µJ pulse energy, the cell-laden bioink was printed successfully. This research study will help to print other retinal neuron cells with collagen I in the LIFT system and show the way of constructing layer-by-layer different cell lines that will help to fabricate the retina ultimately.

Keywords: Laser-Induced Forward Transfer (LIFT), Bioprinting, Collagen I, Design of Experiment (DoE), Cell-laden Bioink.

1. Introduction

Bioprinting is a modified form of the 3D printing process that allows the construction of structures layer by layer by depositing biomaterials mixed with cells for the fabrication of tissues and organs [1]. It has emerged as an efficient method for constructing functional tissues and organs to replace the wounded or diseased tissues [2]. There are several bioprinting techniques such as continuous line-based bioprinting, droplet-based bioprinting, etc. [3]. Droplet-based bioprinting technologies, particularly, Laser-assisted bioprinting and inkjet-based bioprinting are commonly used for getting high-resolution printing [4].

Laser-Induced Forward Transfer (LIFT), a laser direct-write technique, is a novel technique to microfabricate cell-laden biological materials with good cell viability[5]. With this method, high-resolution circular microdroplets with cells can be deposited with proper irradiation parameters [6]. In a LIFT process, a donor substrate is coated with a thin layer of biomaterials on the bottom side and is kept closer to a receiving substrate; a pulsed laser is passed through a laser transparent donor and transfers the material to the receiver [7]. Due to the different rheological and mechanical properties of biomaterials, bad quality printing or non-reproducibility can occur [8]. So, it is very important to optimize the printing parameters to control and reproduce the droplets. To form a successful, smooth, and

high-resolution deposition, several laser properties like laser pulse fluence, pulse energy, pulse width, laser spot size, wavelength as well as material viscosity, coating thickness, and the distance between the donor and acceptor have a major effect [9]

In the field of retina research, LIFT is a promising tool for constructing retinal layers and delivering therapeutic agents directly to the retina.. Due to different types of retinal diseases such as glaucoma, age-related macular degeneration (AMD), diabetic retinopathy etc., more than ten million people are about to blind in the US, and a tremendous number of people are in a threat of diseases [10]. Several types of retinal diseases (retinitis pigmentosa [11], retinal detachment [12], AMD [13], etc.) are primarily related to the retinal photoreceptors cells' loss. But the damage to the photoreceptors does not necessarily lead to loss of the remaining retina or the axons that connect the retina to the brain. In this case, if the photoreceptors could be replaced and innervate the retina accurately, some degree of vision might be recovered [14]. Researchers have been trying to form the layers of photoreceptor cells in vitro so that they can be transplanted. Several experiments have been performed to create the layer of retinal pigment epithelial (RPE) cells [15], [16], rod cells [17], retinal ganglion cells, glial cells [18], etc. Cone cells are one of the two photoreceptor cells, but these cells have not been investigated in LIFT yet. There are some challenges to printing cone cells using LIFT. Precise control of the laser parameters is required to ensure that the cone cells are not damaged during the printing process. Cone cells are highly sensitive to their microenvironment, and any disruption in their extracellular matrix can affect their viability and function [18].

Proper biomaterial selection is also very important for a successful deposition [19]. Particularly, biomaterials such as collagen [20], hyaluronic acid, [21], alginate [22,23], and the mixture of different biomaterials like methylcellulose and hyaluronic acid [21], etc. have been used due to the convenience of printing through the LIFT method. Different mixtures of biomaterials have been used in bioprinting of retinal neuron cells to get proper strength for printing as well as to ensure the actual environment for cell interaction. Isaacson et al. used collagen-based hydrogel containing encapsulated corneal keratocytes cells to print the cornea through the extrusion method [24]. A mixture of collagen and retinal decellularized extracellular matrix (RdECM) was investigated for 3D bioprinting of retinal muller cells using extrusion methods [25]. Eamegdool et al. investigated the growth of RPE cells in different extracellular matrix (ECM) such as collagen I, collagen IV, and nitrite-modified ECM [26]. A thin layer of collagen I successfully maintained the usual activity of RPE cells [27]. Collagen is present in all the connective tissues in the body [28]. It is a suitable biomaterial to make the scaffold for facilitating all types of cell growth and is used in bioprinting of cornea [24], RPE layer of the retina [26], bone tissue [29], aortic heart valve [30], neuron stem cells(which generated axon) [31], and so on. Due to its excellent biocompatibility and weak antigenicity, collagen is used profoundly in tissue engineering [32]. Although more than 28 types of collagens have been found in the body, Type I collagen has covered 80-85 percent of it [33]. Collagen particularly Collagen I, laminin, and fibronectin are the common ECM found in the retina [34]. Very few people have humoral immunity against collagen I and due to this, collagen I is suitable for bioprinting [28]. Since a very small amount of collagen is transferred through the LIFT technique, the collagen droplet tends to dry very quickly. Glycerol is a safe additive for the human body that can be mixed to resist the quick solidification of collagen and to increase printability [35]

However, it is necessary to find out the printability of these cells via 3D bioprinting in vitro so that all the neuron cells can be printed together to mimic the function of a whole retina in the future. But the process parameters are material-specific since the viscosity, surface tension, etc., properties vary from material to material. In the case of retinal neuron cells bioprinting, several techniques such as the extrusion process [17], inkjet techniques [36], and some used laser-assisted techniques [37] were used. The extrusion process lacked precise and controlled deposition of the bioink. Inkjet technique is only suitable for printing low viscosity bioinks, which limits the range of printable materials. Still the optimum printing techniques have not been achieved due to variations of different process parameters. There is still a gap to find out suitable biomaterials and printing strategies during printing and post-printing neuron cells' survival.

In this research, suitable biomaterial composition has been investigated for cone cells to support printability and maintain cell survival functionalities during and after the printing process. Moreover, considering the cell damage during and after the printing process, the appropriate femtosecond laser-based printing strategy for printing the cone cell-laden bioink has been explored.

2. Materials and Methods

2.1. Bioink Preparation

Different concentration of collagen I and glycerol was mixed to obtain a suitable biomaterial for this research.. To find out the proper concentration, we prepared several concentrations from 0.5 mg/ml to 2mg/ml collagen I and tested them in the LIFT system. Higher than 1 mg/ml concentration of collagen I was found challenging to print in our LIFT configuration due to the high viscosity. Glycerol (50% v/v) was mixed with collagen I to resist the quick drying of collagen I during printing. Mouse cone photoreceptor cell line (661w cell line) was mixed with bioink in a ratio of 1 million per milliliter solution and Gibco DMEM/F-12 (Dulbecco's Modified Eagle Medium) was used as a media for the cell line [38]. After preparing several samples without mixing cells, those were tested in the LIFT process and six different concentration was identified as the prospective sample.

2.2. Bioprinting Process

Basically, LIFT is a direct material deposition technique. The LIFT configuration in Biomanufacturing Lab at UTRGV (Fig. 1) consisted of a laser assembly system (Wavelength-1040 nm, output power > 8w, pulse width < 400 fs, repetition rate- 200 kHz supplied by Spirit One 1040-8), a high-speed

front view camera (Phantom ® VEO 401L monochrome high-speed camera) to monitor and record the printing process, a Laser system, a galvanometric scanner, and a computer-controlled three-axis motion stages. There were two coplanar plates: one coplanar plate was known as a donor or print ribbon, which contains the energy-absorbing materials and biomaterials with/without cells to be transported. At the same time, the other one was called the acceptor or receiving substrate in which the materials were deposited (Fig 2). The bottom of the donor was coated with two thin layers; the first was an energy-absorbing layer (1 wt% liquid graphene) [39], while the other one was a transfer layer (collagen I bioink). A 0.5 mm gap was ensured between donor and acceptor (Figure 3). A pulse from the laser was passed through the transparent donor, which volatilized the energy absorbing layer, and a vapor bubble formed as well as expanded gradually. At the same time, the transfer layer expanded also. In one stage, the inner pressure of the bubble became less than the outer pressure, and it started to collapse. Due to inertia and surface tension, the biomaterial could not stick with the energy-absorbing layer and fell to the acceptor. To get a desired structure or pattern, the donor and acceptor are required to move along the x-y axis or scan the laser beam over the donor (usually with galvanometric mirror scanners) [7]. As previously mentioned, several process parameters such as laser pulse fluence, pulse energy, pulse width, laser spot size, the wavelength, etc. as well as other properties like the viscosity of the transfer layer, the coating thickness of the energy-absorbing layer, and the biomaterial, distance between the Donor and Acceptor are required to control for getting a successful, smooth and high-resolution deposition [21]. Some of these parameters such as pulse energy, pulse pick divider etc., have been analyzed in this research.

2.3. Cell viability analysis in Bioink

Cell viability is a significant factor in bioprinting. Since cells become alive if there is proper nutrition and a suitable environment, it is vital to observe the cell viability in the bioink in different time zone [40]. Cell viability is the proportion of live cells within a population [41]. Cell viability can be analyzed in various ways: live/dead staining, ATP(Adenosine triphosphate) detection from cells, evaluation of cell organelle functions, etc. [42]. A live/dead staining kit named Invitrogen™ LIVE/DEAD™ Cell Imaging Kit (488/570) was

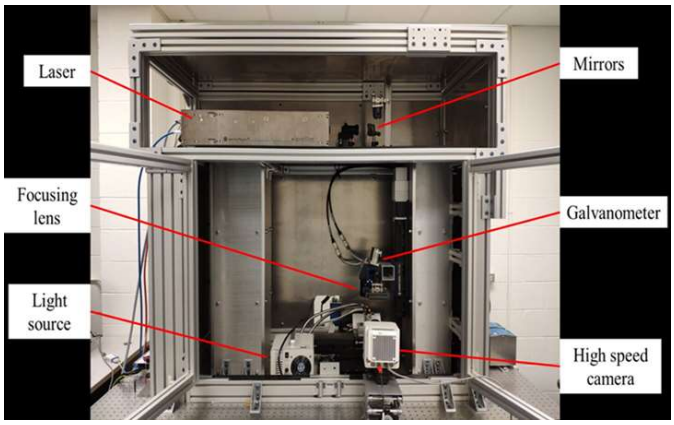

Fig. 1. LIFT Assembly in Biomanufacturing Lab at UTRGV.

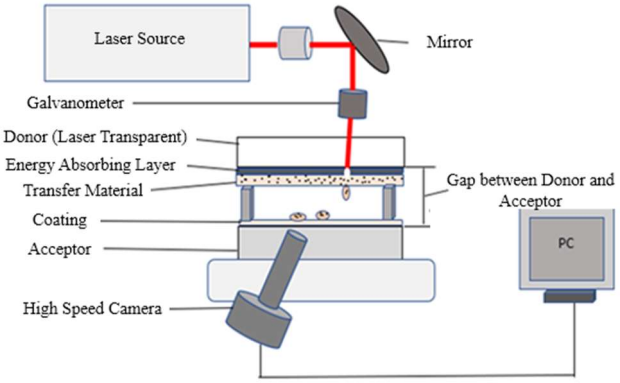

Fig. 2. Schematic diagram of a LIFT method.

purchased from ThermoFisher scientific and used to analyze the cell viability. It was a fluorescent staining kit that was mixed with different cone cell-laden bioink in different time horizons, such as 3hr., 6hr., 9hr., 12hr., and 24hr. Then, it was observed in a confocal microscope with fluorescence light (Nikon AX Confocal Microscope System). A glittering green fluorescence (ex/em 488 nm/515 nm) was produced by the kit indicating the live cells and the sparkling red fluorescence (ex/em 570nm/602 nm) demonstrated the dead cells. Six different concentration of collagen I and glycerol was chosen for cell viability test: 1mg/ml collagen I, 1mg/ml collagen I & 75% glycerol (1:1 ratio), 1mg/ml collagen I & 50% glycerol (1:1 ratio), 0.75mg/ml collagen I, 0.75mg/ml collagen I & 75% glycerol (1:1 ratio), and 0.75 mg/ml collagen I & 50% glycerol (1:1 ratio).Cells were mixed in 1 ml/million ratio with the bioink [18]. To analyze the cell viability, images of the same area were taken with the green and red laser. After that, the glittering green and red cells were counted through the ImageJ software and the proportion of the live cells was calculated.

2.4. Design of Experiment (DoE)

In every research work, a well-structured experimental design helps the research move towards the goal successfully. Design of Experiment (DoE) is a statistical tool to systematically analyze the data, and it is widely used to solve the various optimization problems. The full factorial design was used in this research in which there were three factors: concentration of the bioink mixture, pulse pick divider (a pulse factor for fast pulse selection), and pulse energy (energy emitted by a single pulse). Each factor had four levels. Four levels of concentrations were 1mg/ml collagen I & 50% glycerol mixed (collagen and glycerol were mixed with a 1: 1 ratio using a stirrer), 1mg/ml Collagen I & 50% glycerol unmixed (there was no mixture: first, the collagen I was coated on the donor slide and then, the glycerol was coated), 0.75 mg/ml collagen I & 50% glycerol mixed and 0.75 mg/ml collagen I & 50% glycerol unmixed. Pulse energy had also four levels: 14µJ, 15µJ, 16µJ & 17µJ and the four levels of the pulse pick divider were 8500, 9000, 9500, and 10000. Before setting up the pulse energy range from 14 µJ to 17µJ and pulse pick divider 8500 to 10000, several trial and error was performed. For two concentrations of materials (0.75 mg/ml collagen I & 50% glycerol mixed and 0.75 mg/ml collagen I & 50% glycerol

unmixed), there was no droplet if the pulse energy was less than 12 μJ and the liquid splashed in 17 μJ. For the other two concentration, the minimum threshold energy was 14 μJ and maximum was 18 μJ. Since 14 μJ to 17μJ worked for all four concentrations, 14μJ, 15μJ, 16μJ & 17μJ were chosen as four levels of pulse energy. Applying the same trial and error methods, 8500, 9000, 9500 and 10000 were found suitable four levels for pulse pick divider. Sixty-four different combinations (sixteen different combinations for each concentration of collagen I and glycerol) were generated in Minitab 19 and using those combinations, sixty-four different lines formed in the LIFT process in which some lines were formed by separate droplets, and some were continuous. Then, the average droplet diameter (three droplets from each line was considered or line width for the case where the droplets merged together and formed a continuous line) and the average distance between the edge of two droplets were calculated through ImageJ software. After that, the droplet diameter and distance between the edge of two droplets were placed in the Minitab 19 and the general factorial was analyzed.

3. Results & Discussion

The results of the cell viability analysis were shown in Table 1. Analyzing the cell viability, it was clear that most of the cells were alive at the beginning except for the 1mg/ml collagen mixed with 75% glycerol and 0.75 mg/ml Collagen I with 75% glycerol. Since these two concentrations contained very low living cells, these two were excluded from the bioprinting in the LIFT process.

Table 1. Cell viability analysis in different concentrations of bioink in various time horizons.

Bioink	0.5 hr.	3.0 hr.	6.0 hr.	9.0 hr.	12.0 hr.	24.0 hr.
1 mg/ml Collagen I	90%	81%	77%	42%	35%	18%
1 mg/ml Collagen I & 75% glycerol	41%	22%	21%	16%	10%	0%
1 mg/ml Collagen I & 50% glycerol	88%	79%	48%	21%	11%	2%
0.75 mg/ml Collagen I	89%	71%	56%	46%	30%	17%
0.75 mg/ml Collagen I & 75% glycerol	26%	22%	18%	8%	7%	0%
0.75 mg/ml Collagen I & 50% glycerol	79%	70%	39%	18%	13%	0%

The input and output parameters are given from Table 2 to Table 5.

Table 2. Sixteen input parameters and their corresponding output for 1 mg/ml Collagen I and 50% glycerol unmixed

	Input		Output	
Trial No.	Pulse Energy (μJ)	Pulse Pick Divider	Droplet Diameter (μm)	Distance Between the edge of two droplets (μm)
1	14	8500	139.785	23.711
2	15	8500	147.431	21.968
3	16	8500	172.076	16.48
4	17	8500	128.554	0
5	14	9000	131.661	18.877
6	15	9000	142.413	16.249
7	16	9000	141.935	26.284
8	17	9000	134.767	22.138
9	14	9500	123.18	15.771
10	15	9500	148.387	29.391
11	16	9500	178.495	33.789
12	17	9500	172.521	0
13	14	10000	145.759	21.083
14	15	10000	170.848	33.772
15	16	10000	165.352	27.203
16	17	10000	167.981	34.628

Table 3. Sixteen input parameters and their corresponding output for 1 mg/ml Collagen I and 50% glycerol mixed

	Input		Output	
Trial No.	Pulse Energy (μJ)	Pulse Pick Divider	Droplet Diameter (μm)	Distance Between the edge of two droplets (μm)
1	14	8500	109.14	13.441
2	15	8500	110.088	1.339
3	16	8500	122.381	16.153
4	17	8500	128.75	0
5	14	9000	98.975	8.916
6	15	9000	129.988	1.837
7	16	9000	120	3.631
8	17	9000	96.422	0
9	14	9500	130.153	14.044
10	15	9500	129.384	10.657
11	16	9500	157.593	7.557
12	17	9500	152.817	0
13	14	10000	171.92	44.186
14	15	10000	136.494	23.25
15	16	10000	150.701	0
16	17	10000	150.893	0

Table 4. Sixteen input parameters and their corresponding output for 0.75 mg/ml Collagen I and 50% glycerol unmixed

	Input		Output	
Trial No.	Pulse Energy (μJ)	Pulse Pick Divider	Droplet Diameter (μm)	Distance Between the edge of two droplets (μm)
1	14	8500	154.122	20.310
2	15	8500	176.105	13.768
3	16	8500	198.805	15.361
4	17	8500	201.911	18.189
5	14	9000	140.741	20.313
6	15	9000	170.131	22.613
7	16	9000	168.937	24.707
8	17	9000	172.76	26.095
9	14	9500	104.898	33.453
10	15	9500	131.9	27.535
11	16	9500	151.015	11.469

12	17	9500	138.829	20.81
13	14	10000	130.227	38.709
14	15	10000	118.041	9.319
15	16	10000	132.14	16.009
16	17	10000	129.988	35.831

Table 5 Sixteen input parameters and their corresponding output for 0.75 mg/ml Collagen I and 50% glycerol mixed.

	Input		Output	
Trial No.	Pulse Energy (μJ)	Pulse Pick Divider	Droplet Diameter (μm)	Distance Between the edge of two droplets (μm)
1	14	8500	134.265	25.329
2	15	8500	148.865	32.981
3	16	8500	142.891	13.01
4	17	8500	121.386	0
5	14	9000	99.164	42.533
6	15	9000	114.696	34.170
7	16	9000	145.042	14.337
8	17	9000	109.438	14.098
9	14	9500	83.871	16.461
10	15	9500	113.978	16.488
11	16	9500	123.536	19.363
12	17	9500	125.462	11.708
13	14	10000	81.005	21.281
14	15	10000	107.766	12.872
15	16	10000	119.474	10.991
16	17	10000	178.698	18.601

ANOVA (analysis of variance) table of the output parameters was found after analyzing the table 2 to table 4 data, which indicates the relationship between the output and input parameters. In the ANOVA table, there were degree of freedom (DF), adjusted sum of squared (Adj SS) value, adjusted mean squared (Adj MS) value, F-value, and P-value. In this study, the standard 95% confidence interval was chosen for the statistical analysis. So, α=0.05, and if the p-value of the factor is less than 0.05, it will be a significant parameter. The ANOVA table for droplet diameter or line width and the distance between the edge of two droplets are shown in Tables 6 and 7, respectively.

Table 6. ANOVA table for droplet diameter or line width

Source	DF	Adj SS	Adj MS	F-Value	P-Value
Model	36	36245	1006.8	3.97	0.000
Linear	9	18117	2013.0	7.94	0.000
Con. of collagen I and glycerol	3	10335	3444.9	13.60	0.000
Pulse Pick Divider	3	1780	593.4	2.34	0.096
Pulse Energy	3	6002	2000.7	7.90	0.001
2-Way Interactions	27	18128	671.4	2.65	0.007
Con. of collagen I and glycerol*Pulse Pick Divider	9	13953	1550.3	6.12	0.000
Con. of collagen I and glycerol*Pulse Energy	9	1401	155.7	0.61	0.774
Pulse Pick Divider*Pulse Energy	9	2774	308.2	1.22	0.326
Error	27	6841	253.4		
Total	63	43086			

Table 7. ANOVA table for the distance between the edge of two droplets

Source	DF	Adj SS	Adj MS	F-Value	P-Value
Model	36	6096.0	169.33	1.95	0.038
Linear	9	3496.6	388.51	4.47	0.001
Con. of collagen I and glycerol	3	1939.4	646.46	7.43	0.001
Pulse Pick Divider	3	475.3	158.42	1.82	0.167
Pulse Energy	3	1081.9	360.65	4.15	0.015
2-Way Interactions	27	2599.4	96.27	1.11	0.397
Con. of collagen I and glycerol*Pulse Pick Divider	9	776.3	86.25	0.99	0.470
Con. of collagen I and glycerol*Pulse Energy	9	1173.4	130.38	1.50	0.199
Pulse Pick Divider*Pulse Energy	9	649.6	72.18	0.83	0.595
Error	27	2348.4	86.98		
Total	63	8444.3			

Table 6 showed that the p-value of concentration of collagen I and glycerol and pulse energy and one two-way interaction between the concentration of collagen I and glycerol & pulse pick divider was less than 0.05. So, the concentration of the materials and pulse energy were statistically significant for droplet diameter. In the case of the distance between the edge of two droplets, the result was also the same. The concentration of collagen I and glycerol and pulse energy were significant as their p-value is less than 0.05 (Table 7).

Analyzing the general full factorial design with sixty-four experimental data, it was found that with the increase of pulse energy, droplet sizes and distance between the edge of two droplets were increased in most cases. For the concentration of materials, unmixed collagen I and glycerol generated larger average droplets and longer distances than the mixed one. Although droplet sizes and distance between the edge of two droplets were increased with the increase of the pulse pick divider, it was not statistically significant. However, the relationship among the parameters was non-linear and it was infeasible to deduce the linear regression equation. From the DoE analysis and their images from fig. 3 to fig. 6, it was seen that 15 μJ and 16μJ pulse energy and 9500 pulse pick divider produced stable droplets with a mean diameter ranging from 135 μm to 150 μm. Moreover, the unmixed collagen I and glycerol had longer cell viability. Hence, the cells were mixed

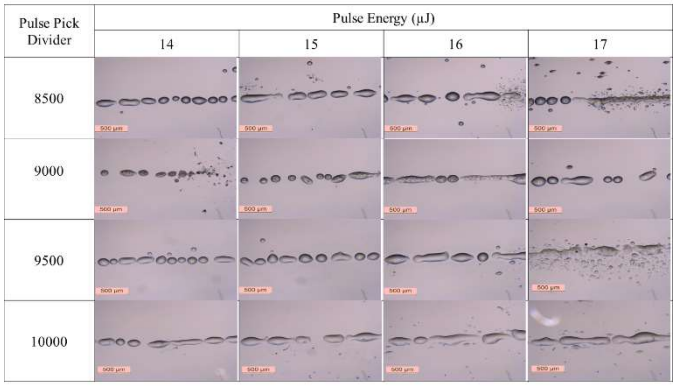

Fig.3. Printed droplets by LIFT technique for 1mg/ml Collagen I and 50% glycerol unmixed.

with the unmixed collagen I and then a coating of glycerol was provided to it.

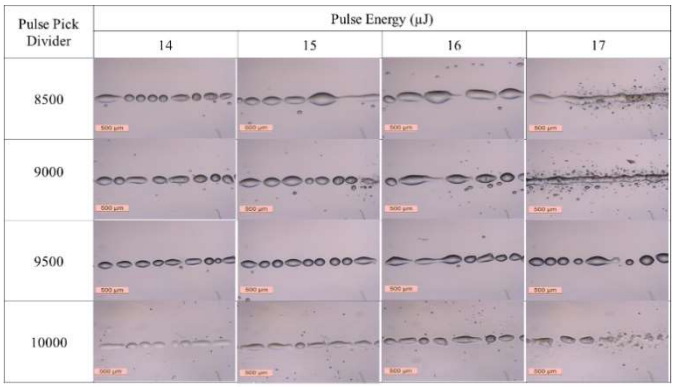

Fig. 4. Printed droplets by LIFT technique for 1mg/ml Collagen I and 50% glycerol mixed

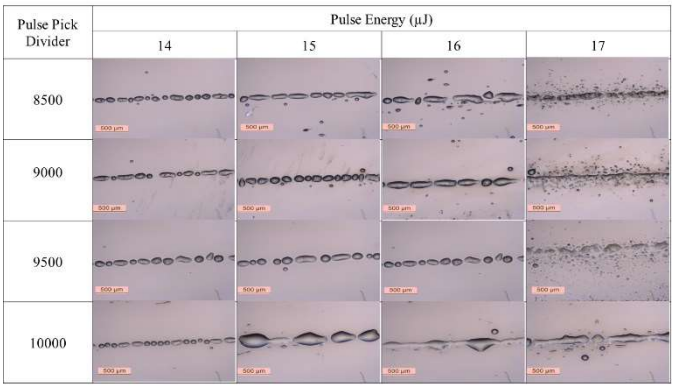

Fig. 5. Printed droplets by LIFT technique for 0.75mg/ml Collagen I and 50% glycerol unmixed

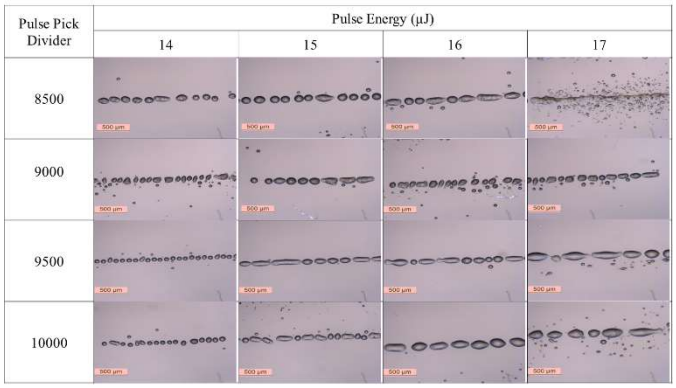

Fig. 6. Printed droplets by LIFT technique for 0.75mg/ml Collagen I and 50% glycerol mixed

The cone cells' average length was observed approximately 130 µm to 160 µm in fresh media after three days in the lab (Fig. 7). So, 15 µJ and 16µJ pulse energy with 9500 pulse pick divider were used so that the droplets could be large enough to grow the cells into it. The images of the droplets with cone cells were shown in Fig. 8 to 11. Since there was very little control on cell mixtures with bioink, all the cells were not spread in the bioink evenly. Hence, the cells in each droplet varied such as some droplets contained three-four cells, some contained more than that and some had no cells in them. Though the bioink was printed successfully, the cell viability was very poor. Most of the cells were found dead in the printed droplet 2 hrs. after printing (Fig. 12 and 13).

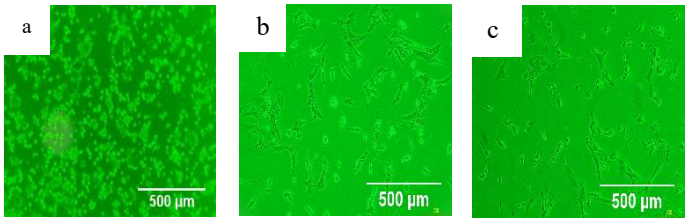

Fig. 7. Mouse cone cell growth in Gibco DMEM/F-12 Media on (a) Day 1, (b) Day 2, and (c) Day 3

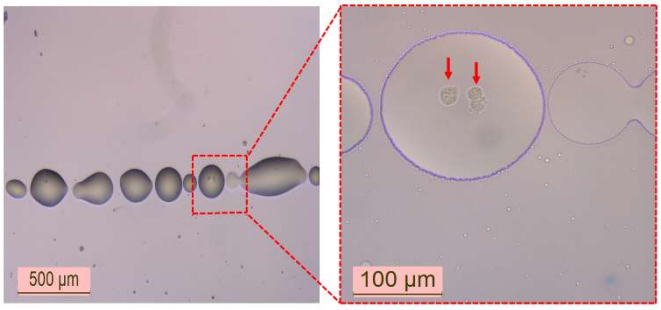

Fig. 8. Printed droplets with cells using pulse energy 15 µJ and pulse pick divider 9500 for 1mg/ml Collagen I and 50% glycerol unmixed

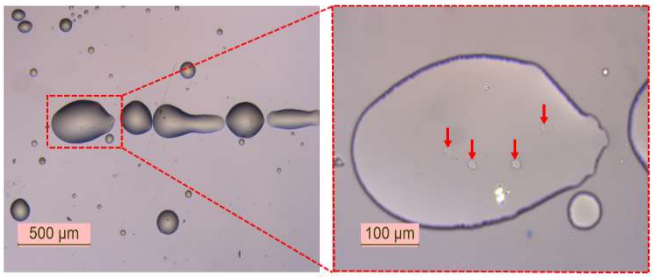

Fig. 9. Printed droplets with cells using pulse energy 16 µJ and pulse pick divider 9500 for 1mg/ml Collagen I and 50% glycerol unmixed

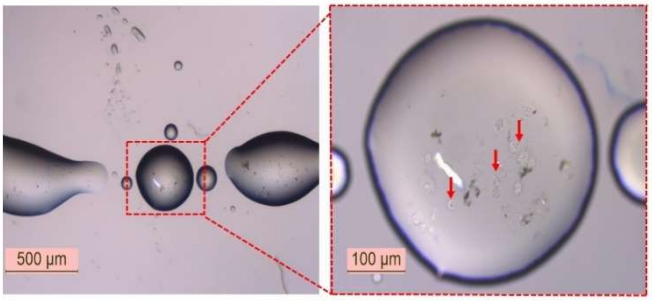

Fig. 10. Printed droplets with cells using pulse energy 15 µJ and pulse pick divider 9500 for 0.75mg/ml Collagen I and 50% glycerol unmixed.

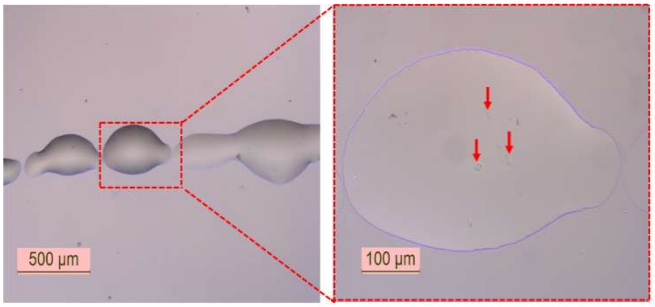

Fig. 11. Printed droplets with cells using pulse energy 16 µJ and pulse pick divider 9500 for 0.75mg/ml Collagen I and 50% glycerol unmixed

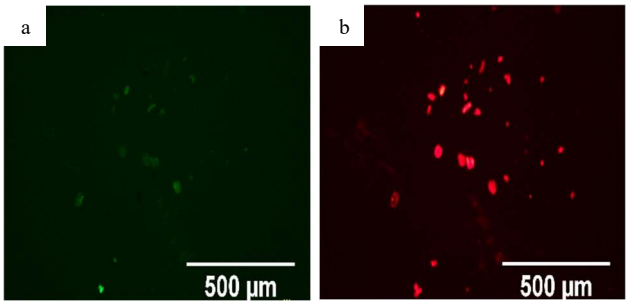

Fig. 12. Fluorescence Image of cell-laden droplet sample of 1mg/ml collagen I and 50% glycerol unmixed. (a) bright green dots indicate live cells (b) bright red dots indicate dead cells.

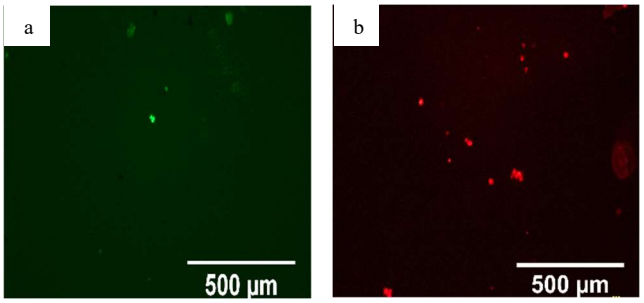

Fig. 13. Fluorescence Image of cell-laden droplet sample of 0.75mg/ml collagen I and 50% glycerol unmixed. (a) bright green dots indicate live cells (b) bright red dots indicate dead cells.

The drop-by-drop lines & continuous lines were formed successfully using collagen Ⅰ and glycerol through the LIFT method. Cell viability analysis provided information about the cell survival in the bioink a few hours outside the incubator which indicated the capability of printing the cell-laden bioink in the LIFT system. The statistical analysis revealed that pulse energy was the most significant process parameter. With the increase of pulse energy, the droplet size increased, and the distance between the edge of two droplets decreased. But it happened for a certain energy level, and in one stage, the splashes of bioink were observed due to the high energy.

Analyzing the DoE, some values of these parameters have been identified, and using those parameters, cell-laden bioink was printed successfully. But the cell viability was comparatively lower in the biomaterials and most of the cells died after printing. The unavailability of the biosafety cabinet and incubator near the LIFT printing facility made it difficult to transfer the printed cells to an environment suitable for living. The cell viability could be increased if there was a controllable environment.

4. Conclusion

In this study, mouse cone photoreceptor cell-laden bioink has been printed successfully through the LIFT process. Since the cell viability was low, it should be increased in bioprinted lines in the future. The environment (such as dust, airflow, temperature, etc.) should be controlled so that the contamination can be minimized, and cells can get a convenient environment for living. A biosafety cabinet around the LIFT system might help to ensure a suitable environment. Capabilities of layer-by-layer bioprinting have to be achieved also as we have been able to print only a single line until now. Computer-controlled pattern design or path patterning system will help to create a 3D structure in this printer. It is also required to analyze the cell morphology in the bioprinted sample thoroughly. Moreover, an even and thin coating of bioink on the donor must be ensured for getting stable droplets and continuous lines. Finally, this study will help to identify the printability of cell-laden collagen bioink in the LIFT system and will assist to print layer-by-layer neuron cells of the retina in the future.

Acknowledgements

This work was supported by the U.S. Department of Defense Manufacturing Engineering Education Program (MEEP) program under Award No. N00014–19-1–2728, the Bose Family Donation to the Department of Manufacturing and Industrial Engineering at UTRGV.

The authors declare that they have no known competing financial interests or personal relationships that could have appeared to influence the work reported in this paper.

References

[1] Panja N, Maji S, Choudhuri S, Ali KA, Hossain CM. 3D Bioprinting of Human Hollow Organs. AAPS PharmSciTech 2022;23:139. https://doi.org/10.1208/s12249-022-02279-9.

[2] Gungor-Ozkerim PS, Inci I, Zhang YS, Khademhosseini A, Dokmeci MR. Bioinks for 3D bioprinting: an overview. Biomaterials Science 2018;6:915–46. https://doi.org/10.1039/C7BM00765E.

[3] Murphy SV, Atala A. 3D bioprinting of tissues and organs. Nature Biotechnology 2014;32:773–85. https://doi.org/10.1038/nbt.2958.

[4] Ke D, Niu C, Yang X. Evolution of 3D bioprinting-from the perspectives of bioprinting companies. Bioprinting 2022;25:e00193. https://doi.org/10.1016/j.bprint.2022.e00193.

[5] Guillemot F, Souquet A, Catros S, Guillotin B, Lopez J, Faucon M, et al. High-throughput laser printing of cells and biomaterials for tissue engineering. Acta Biomaterialia 2010;6:2494–500. https://doi.org/10.1016/j.actbio.2009.09.029.

[6] Guillotin B, Souquet A, Catros S, Duocastella M, Pippenger B, Bellance S, et al. Laser assisted bioprinting of engineered tissue with high cell density and microscale organization. Biomaterials 2010;31:7250–6. https://doi.org/10.1016/j.biomaterials.2010.05.055.

[7] Dias AD, Kingsley DM, Corr DT. Chapter 5 - Engineering 2D and 3D Cellular Microenvironments Using Laser Direct Write. In: Zhang LG, Fisher JP, Leong KW, editors. 3D Bioprinting and Nanotechnology in Tissue Engineering and Regenerative Medicine, Academic Press; 2015, p. 105–27. https://doi.org/10.1016/B978-0-12-800547-7.00005-9.

[8] Pugliese R, Beltrami B, Regondi S, Lunetta C. Polymeric biomaterials for 3D printing in medicine: An overview. Annals of 3D Printed Medicine 2021;2:100011. https://doi.org/10.1016/j.stlm.2021.100011.

[9] Morales M, Munoz-Martin D, Marquez A, Lauzurica S, Molpeceres C. Chapter 13 - Laser-Induced Forward Transfer Techniques and Applications. In: Lawrence J, editor. Advances in Laser Materials Processing (Second Edition), Woodhead Publishing; 2018, p. 339–79. https://doi.org/10.1016/B978-0-08-101252-9.00013-3.

[10] Common Eye Disorders and Diseases \textbar CDC 2020.

[11] Noel NCL, MacDonald IM. RP1L1 and inherited photoreceptor disease: A review. Survey of Ophthalmology 2020;65:725–39. https://doi.org/10.1016/j.survophthal.2020.04.005.

[12] Murakami Y, Notomi S, Hisatomi T, Nakazawa T, Ishibashi T, Miller JW, et al. Photoreceptor cell death and rescue in retinal detachment and degenerations. Progress in Retinal and Eye Research 2013;37:10.1016/j.preteyeres.2013.08.001. https://doi.org/10.1016/j.preteyeres.2013.08.001.

[13] van Asten F, Simmons M, Singhal A, Keenan TD, Ratnapriya R, Agrón E, et al. A Deep Phenotype Association Study Reveals Specific Phenotype Associations with Genetic Variants in Age-related Macular Degeneration: Age-Related Eye Disease Study 2 (AREDS2) Report No. 14. Ophthalmology 2018;125:559–68. https://doi.org/10.1016/j.ophtha.2017.09.023.

[14] Barber AC, Hippert C, Duran Y, West EL, Bainbridge JWB, Warre-Cornish K, et al. Repair of the degenerate retina by photoreceptor transplantation. Proceedings of the National Academy of Sciences of the United States of America 2013;110:354–9. https://doi.org/10.1073/pnas.1212677110.

[15] Heidari R, Soheili Z-S, Samiei S, Ahmadieh H, Davari M, Nazemroaya F, et al. Alginate as a cell culture substrate for growth and differentiation of human retinal pigment epithelial cells. Applied Biochemistry and Biotechnology 2015;175:2399–412. https://doi.org/10.1007/s12010-014-1431-z.

[16] Tan EYS, Agarwala S, Yap YL, Tan CSH, Laude A, Yeong WY. Novel method for the fabrication of ultrathin, free-standing and porous polymer membranes for retinal tissue engineering. Journal of Materials Chemistry B 2017;5:5616–22. https://doi.org/10.1039/C7TB00376E.

[17] Shi P, Edgar TYS, Yeong WY, Laude A. Hybrid three-dimensional (3D) bioprinting of retina equivalent for ocular research. International Journal of Bioprinting 2017;3:008. https://doi.org/10.18063/IJB.2017.02.008.

[18] Lorber B, Hsiao W-K, Hutchings IM, Martin KR. Adult rat retinal ganglion cells and glia can be printed by piezoelectric inkjet printing. Biofabrication 2013;6:015001. https://doi.org/10.1088/1758-5082/6/1/015001.

[19] Fu Z, Ouyang L, Xu R, Yang Y, Sun W. Responsive biomaterials for 3D bioprinting: A review. Materials Today 2022;52:112–32. https://doi.org/10.1016/j.mattod.2022.01.001.

[20] Keriquel V, Oliveira H, Rémy M, Ziane S, Delmond S, Rousseau B, et al. In situ printing of mesenchymal stromal cells, by laser-assisted bioprinting, for in vivo bone regeneration applications. Scientific Reports 2017;7:1778. https://doi.org/10.1038/s41598-017-01914-x.

[21] Yusupov V, Churbanov S, Churbanova E, Bardakova K, Antoshin A, Evlashin S, et al. Laser-induced Forward Transfer Hydrogel Printing: A Defined Route for Highly Controlled Process. International Journal of Bioprinting 2020;6:271. https://doi.org/10.18063/ijb.v6i3.271.

[22] Koch L, Deiwick A, Schlie S, Michael S, Gruene M, Coger V, et al. Skin tissue generation by laser cell printing. Biotechnology and Bioengineering 2012;109:1855–63. https://doi.org/10.1002/bit.24455.

[23] Kingsley D, Dias A, Chrisey D, Corr D. Single-step laser-based fabrication and patterning of cell-encapsulated alginate microbeads. Biofabrication 2013;5:045006. https://doi.org/10.1088/1758-5082/5/4/045006.

[24] Isaacson A, Swioklo S, Connon CJ. 3D bioprinting of a corneal stroma equivalent. Experimental Eye Research 2018;173:188–93. https://doi.org/10.1016/j.exer.2018.05.010.

[25] Kim J, Kong JS, Kim H, Han W, Won JY, Cho D-W. Maturation and Protection Effect of Retinal Tissue-Derived Bioink for 3D Cell Printing Technology. Pharmaceutics 2021;13:934. https://doi.org/10.3390/pharmaceutics13070934.

[26] Eamegdool SS, Sitiwin EI, Cioanca AV, Madigan MC. Extracellular matrix and oxidative stress regulate human retinal pigment epithelium growth. Free Radical Biology & Medicine 2020;146:357–71. https://doi.org/10.1016/j.freeradbiomed.2019.11.018.

[27] Abedin Zadeh M, Khoder M, Al-Kinani AA, Younes HM, Alany RG. Retinal cell regeneration using tissue engineered polymeric scaffolds. Drug Discovery Today 2019;24:1669–78. https://doi.org/10.1016/j.drudis.2019.04.009.

[28] Sensharma P, Madhumathi G, Jayant RD, Jaiswal AK. Biomaterials and cells for neural tissue engineering: Current choices. Materials Science and Engineering: C 2017;77:1302–15. https://doi.org/10.1016/j.msec.2017.03.264.

[29] Li Z, Du T, Ruan C, Niu X. Bioinspired mineralized collagen scaffolds for bone tissue engineering. Bioactive Materials 2021;6:1491–511. https://doi.org/10.1016/j.bioactmat.2020.11.004.

[30] Maxson EL, Young MD, Noble C, Go JL, Heidari B, Khorramirouz R, et al. In vivo remodeling of a 3D-Bioprinted tissue engineered heart valve scaffold. Bioprinting 2019;16:e00059. https://doi.org/10.1016/j.bprint.2019.e00059.

[31] Sun Y, Yang C, Zhu X, Wang J-J, Liu X-Y, Yang X-P, et al. 3D printing collagen/chitosan scaffold ameliorated axon regeneration and neurological recovery after spinal cord injury. Journal of Biomedical Materials Research Part A 2019;107:1898–908. https://doi.org/10.1002/jbm.a.36675.

[32] Chan WW, Yeo DCL, Tan V, Singh S, Choudhury D, Naing MW. Additive Biomanufacturing with Collagen Inks. Bioengineering (Basel) 2020;7:E66. https://doi.org/10.3390/bioengineering7030066.

[33] Felician FF, Xia C, Qi W, Xu H. Collagen from Marine Biological Sources and Medical Applications. Chemistry & Biodiversity 2018;15:e1700557. https://doi.org/10.1002/cbdv.201700557.

[34] Reinhard J, Joachim SC, Faissner A. Extracellular matrix remodeling during retinal development. Experimental Eye Research 2015;133:132–40. https://doi.org/10.1016/j.exer.2014.07.001.

[35] Triyono J, Alfiansyah R, Sukanto H, Ariawan D, Nugroho Y. Fabrication and characterization of porous bone scaffold of bovine hydroxyapatite-glycerin by 3D printing technology. Bioprinting 2020;18:e00078. https://doi.org/10.1016/j.bprint.2020.e00078.

[36] Masaeli E, Forster V, Picaud S, Karamali F, Nasr-Esfahani MH, Marquette C. Tissue engineering of retina through high resolution 3-dimensional inkjet bioprinting. Biofabrication 2020;12:025006. https://doi.org/10.1088/1758-5090/ab4a20.

[37] Roversi K, Ebrahimi Orimi H, Falchetti M, Lummertz da Rocha E, Talbot S, Boutopoulos C. Bioprinting of Adult Dorsal Root Ganglion (DRG) Neurons Using Laser-Induced Side Transfer (LIST). Micromachines 2021;12:865. https://doi.org/10.3390/mi12080865.

[38] Rodriguez RR, Tsin ATC, Keniry M, Lowe K. Acrolein and Hypoxia Induced VEGF Secretion by 661W Cone Photoreceptors. Investigative Ophthalmology & Visual Science 2021;62:2987.

[39] Qu J, Dou C, Xu B, Li J, Rao Z Tsin A. Printing quality improvement for laser-induced forward transfer bioprinting: Numerical modeling and experimental validation. Physics of Fluids 2021;33:071906. https://doi.org/10.1063/5.0054675.

[40] Malekpour A, Chen X. Printability and Cell Viability in Extrusion-Based Bioprinting from Experimental, Computational, and Machine Learning Views. Journal of Functional Biomaterials 2022;13:40. https://doi.org/10.3390/jfb13020040.

[41] Riss TL, Moravec RA, Niles AL, Duellman S, Benink HA, Worzella TJ, et al. Cell Viability Assays. In: Markossian S, Grossman A, Brimacombe K, Arkin M, Auld D, Austin CP, et al., editors. Assay Guidance Manual, Bethesda (MD): Eli Lilly & Company and the National Center for Advancing Translational Sciences; 2004.

[42] Thakare K, Jerpseth L, Qin H, Pei Z. Bioprinting Using Algae: Effects of Extrusion Pressure and Needle Diameter on Cell Quantity in Printed Samples. Journal of Manufacturing Science and Engineering 2020;143. https://doi.org/10.1115/1.4048853.